emeraldinsight

COMPEL - The international journal for computation and mathematics in electrical and electronic engineering

Smart VRP-NLMS algorithm for estimation of power system frequency
Seyed Reza Aali, Mohammad Reza Besmi, Mohammad Hosein Kazemi,

Article information:

To cite this document:
Seyed Reza Aali, Mohammad Reza Besmi, Mohammad Hosein Kazemi, (2018) "Smart VRP-NLMS algorithm for estimation of power system frequency", COMPEL - The international journal for computation and mathematics in electrical and electronic engineering, https://doi.org/10.1108/COMPEL-06-2018-0263
Permanent link to this document:
https://doi.org/10.1108/COMPEL-06-2018-0263

Downloaded on: 02 November 2018, At: 05:58 (PT)
References: this document contains references to 28 other documents.
To copy this document: permissions@emeraldinsight.com
Access to this document was granted through an Emerald subscription provided by
Token: Eprints: QSFUD4JWZFCCVUSDRKGN:

For Authors

If you would like to write for this, or any other Emerald publication, then please use our Emerald for Authors service information about how to choose which publication to write for and submission guidelines are available for all. Please visit www.emeraldinsight.com/ authors for more information.

About Emerald www.emeraldinsight.com

Emerald is a global publisher linking research and practice to the benefit of society. The company manages a portfolio of more than 290 journals and over 2,350 books and book series volumes, as well as providing an extensive range of online products and additional customer resources and services.

Emerald is both COUNTER 4 and TRANSFER compliant. The organization is a partner of the Committee on Publication Ethics (COPE) and also works with Portico and the LOCKSS initiative for digital archive preservation.

*Related content and download information correct at time of download.

Downloaded by SHAHED UNIVERSITY OF MEDICAL SCIENCES, Ms Seyed Reza Aali At 05:58 02 November 2018 (PT)

The current issue and full text archive of this journal is available on Emerald Insight at:
www.emeraldinsight.com/0332-1649.htm

Smart VRP-NLMS algorithm for estimation of power system frequency

Seyed Reza Aali, Mohammad Reza Besmi and Mohammad Hosein Kazemi
Electrical and Electronic Engineering, Shahed University, Tehran, Iran

Received 28 June 2018
Revised 20 August 2018
Accepted 24 September 2018

Downloaded by SHAHED UNIVERSITY OF MEDICAL SCIENCES, Ms Seyed Reza Aali At 05:58 02 November 2018 (PT)

Abstract

Purpose – The purpose of this paper is to study variation regularization with a positive sequence extraction-normalized least mean square (VRP-NLMS) algorithm for frequency estimation in a three-phase electrical distribution system. A simulation test is provided to validate the performance and convergence rate of the proposed estimation algorithm.

Design/methodology/approach – Least mean square (LMS) algorithms for frequency estimation encounter problems when voltage contains unbalance, sags and harmonic distortion. The convergence rate of the LMS algorithm is sensitive to the adjustment of the step-size parameter used in the update equation. This paper proposes VRP-NLMS algorithm for frequency estimation in a power system. Regularization parameter is variable in the NLMS algorithm to adjust step-size parameter. Delayed signal cancellation (DSC) operator suppresses harmonics and negative sequence component of the voltage vector in a two-phase $\hat{I} \pm \hat{I}^2$ plane. The DSC part is placed in front of the NLMS algorithm as a pre-filter and a positive sequence of the grid voltage is extracted.

Findings – By adapting of the step-size parameter, speed and accuracy of the LMS algorithm are improved. The DSC operator is augmented to the NLMS algorithm for more improvement of the performance of this adaptive filter. Simulation results validate that the proposed VRP-NLMS algorithm has a less misalignment of performance with more convergence rate.

Originality/value – This paper is a theoretical support to simulated system performance.

Keywords Adaptive filtering, Delayed signal cancellation (DSC), Frequency estimation, NLMS, Variable regularization

Paper type Research paper

Nomenclature

η	= Step-size parameter;
ε	= Regularization parameter;
ΔT	= Sampling interval;
$\Delta\omega_g$	= Deviation of the grid frequency;
e_k	= Error signal;
$\hat{f}(k)$	= Estimated frequency;
J_k	= Cost function;
ϕ	= Phase of voltage;
T	= Fundamental period;
k	= Time instant;
THD	= Total harmonic distortion;

COMPEL - The international journal for computation and mathematics in electrical and electronic engineering
© Emerald Publishing Limited
0332-1649
DOI 10.1108/COMPEL-06-2018-0263

μ = Step-size coefficient;
$\hat{V}_k$ = Estimated voltage;
ω = Angular frequency;
$\Im_{(\cdot)}$ = Imaginary part of a complex-valued number;
$\Re_{(\cdot)}$ = Real part of a complex-valued number;
$||\underline{V_k}||_2$ = L_2-norm of $\underline{V_k}$;
$||\hat{f}||_2$ = L_2-norm of $\hat{f}$;
DSC = Delayed signal cancellation;
FFPS = Fundamental frequency positive sequence;
FRP = Fixed regularization with a positive-sequence-extraction;
LMS = Least mean square;
NLMS = Normalized LMS;
NMSD = Normalized mean square deviation;
PLL = Phase locked loop; and
VR = Variable regularization.

1. Introduction

Frequency is an important factor in power quality control, protection and synchronizing of power converters connected to the grid. Also, an accurate estimation of system frequency is essential for protection, dynamic control and power system stabilization (Chilipi *et al.*, 2016; He *et al.*, 2017; Li *et al.*, 2017; Smith *et al.*, 2009). Several strategies such as the discrete Fourier transform -based (Xia *et al.*, 2017), a phase-locked loop (PLL) (Ciobotaru *et al.*, 2010), frequency-locked loop (FLL) (Bei and Wang, 2016), Kalman filters (Dini and Mandic, 2013) and Clark's transformation-based frequency measurement (Dash *et al.*, 2000) have been presented for frequency estimation in power systems.

Adaptive filtering is an effective technique in many applications such as system identification, channel equalization, network and acoustic echo cancellation and active noise control. Adaptive filters are established based on minimizing the mean square error and have a simple configuration, less computation, more efficiency and stability and robustness in the presence of noise and harmonic distortions (Chellappa and Theodoridis, 2014; Sayed, 2003; Simon, 2002). Adaptive filters such as least mean squares (LMS) method (Xia and Mandic, 2012), normalized LMS (NLMS) (Sayed, 2003) are prevalent for DSP-based power converters because voltage components calculated via Clark's transformation are already available for synchronizing of network current or power controller loops. Most protection and control applications in power systems need to an accurate and fast estimation of the system frequency. Disturbances including voltage sag, harmonics and unbalance distortion are the major difficulties of frequency estimation (Arablouei *et al.*, 2015; Wang and Li, 2011a, 2011b). Therefore, the conventional LMS and NLMS algorithms will be failed against these disturbances and cannot track the frequency deviations accurately. The performance of the NLMS tends to deteriorate in the presence of negative sequence components in grid voltage.

For overcoming the aforementioned problem, an additional filtering stage is usually added, either before or within the PLL loop. Among filtering strategies, the delayed signal cancellation (DSC) operator is more popular because it can be easily tailored to different grid scenarios. The DSC operator eliminates all orders of harmonics, including DC offset and negative sequence components in highly distorted voltage. The DSC operator extracts the fundamental frequency positive sequence (FFPS) component of the grid voltage. The DSC operator(s) can be used either as an in-loop filter in the PLL structure or as a pre-filter for the PLL input (Golestan *et al.*, 2017; Golestan *et al.*, 2015; Huang and Rajashekara, 2017; Subudhi *et al.*, 2009). The DSC filter has a low computational burden for the implementation and

Downloaded by SHAHED UNIVERSITY OF MEDICAL SCIENCES, Ms Seyed Reza Aali At 05:58 02 November 2018 (PT)

Downloaded by SHAHED UNIVERSITY OF MEDICAL SCIENCES, Ms Seyed Reza Aali At 05:58 02 November 2018 (PT)

ensures a fast dynamic response and high filtering capability. A hybrid adaptive/non-adaptive DSC operators-based PLL for the accurate and fast extraction of the grid voltage parameters was proposed in Golestan *et al* (2017).

In this paper, a combination of a DSC operator with a variable regularization (VR)-NLMS algorithm is presented for fundamental frequency estimation of the power system. The DSC part with a simple complexity is placed in front of the NLMS algorithm as a pre-filter, and a positive sequence of the grid voltage is extracted. The normalized part of NLMS is also changed. The DSC part and VR of the proposed NLMS algorithm change the performance and convergence rate of the adaptive filter.

This paper is organized as follows: Section 2 reviews the NLMS estimation algorithm. The VR-NLMS algorithm is presented in Section 3. Section 4 analyses the stability of the proposed algorithm. The DSC as a pre-filter in the proposed algorithm is stated in Section 5. Section 6 presents simulation results for frequency estimation under distorted conditions, including voltage sags, unbalanced and higher-order harmonics. Finally, Section 7 concludes the paper.

2. Review of normalized least mean squares algorithm

The discretized balanced voltages of a three-phase power system can be represented as:

$$\begin{bmatrix} v_{a,k} \\ v_{b,k} \\ v_{c,k} \end{bmatrix} = \begin{bmatrix} V_a \cos(\omega k \Delta T + \phi) \\ V_b \cos\left(\omega k \Delta T + \phi - \frac{2\pi}{3}\right) \\ V_c \cos\left(\omega k \Delta T + \phi + \frac{2\pi}{3}\right) \end{bmatrix} \tag{1}$$

where $v_{a,k}$, $v_{b,k}$ and $v_{c,k}$ are three-phase voltage at a time instant k. V_a, V_b and V_c are maximal values of the phase voltages. $\Delta T$is the sampling interval, ϕ is the phase of the fundamental component, $\omega = 2\pi f$ is the angular frequency of the voltage signal and $f$is the signal frequency.

The three-phase system can be transformed into a two-phase complex using Clarke's transformation into a zero sequence v_0, and the complex and orthogonal v_α and v_β according to the following equation:

$$\begin{bmatrix} v_{0,k} \\ v_{\alpha,k} \\ v_{\beta,k} \end{bmatrix} = \sqrt{\frac{2}{3}} \begin{bmatrix} \frac{\sqrt{2}}{2} & \frac{\sqrt{2}}{2} & \frac{\sqrt{2}}{2} \\ 1 & -\frac{1}{2} & -\frac{1}{2} \\ 0 & \frac{\sqrt{3}}{2} & -\frac{\sqrt{3}}{2} \end{bmatrix} \begin{bmatrix} v_{a,k} \\ v_{b,k} \\ v_{c,k} \end{bmatrix} \tag{2}$$

The zero-sequence component $v_{0,k}$ is not necessary for analysis, and zero-sequence is in many cases blocked by the transformers; complex voltage is defined by:

$$\underline{V_k} = v_{\alpha,k} + j v_{\beta,k} \tag{3}$$

where $j = \sqrt{-1}$.

Downloaded by SHAHED UNIVERSITY OF MEDICAL SCIENCES, Ms Seyed Reza Aali At 05:58 02 November 2018 (PT)

Underlined letter _ distinct the notation of vectors and scalars (Farhang-Boroujeny, 2013; Mandic and Goh, 2009; Manolakis *et al.*, 2000). The complex voltage can also be written using polar coordinates as:

$$\underline{V_k} = Ae^{(j\omega k\Delta T+\phi)} \tag{4}$$

where A is the estimated amplitude of the complex vector, ω is estimated angular frequency of the voltage.

A new vector value can be expressed in the recursive method using the previous step value. Assuming a constant signal frequency between two signal sample instants results in

$$\underline{V_k} = \underline{V_{k-1}}\, e^{j\omega k\Delta T} \tag{5}$$

This equation is the foundation of the complex recursive LMS algorithm for frequency estimation.

The complex LMS (CLMS) is a natural extension of the real LMS and work on complex nonlinear architectures (Farhang-Boroujeny, 2013; Mandic and Goh, 2009). The CLMS error signal is calculated by using the measured V_k and estimated $\underline{\hat{V}_k}$ voltage vector in k step as:

$$\underline{e_k} = \underline{V_k} - \underline{\hat{V}_k} \tag{6}$$

where $\underline{e_k}$ is the error between input vector and combiner output.

In addition, complex weight vectors will be $\underline{W_{k-1}} = e^{j\hat{\omega}k\Delta T}$, and combiner output (complex voltage vector) is estimated by:

$$\underline{\hat{V}_k} = \underline{W_{k-1}} \,.\, \underline{\hat{V}_{k-1}} \tag{7}$$

The weight vector of CLMS is calculated recursively using

$$\underline{W_k} = \underline{W_{k-1}} + \mu \underline{e_{k-1}}\, \underline{V^*_{k-1}} \tag{8}$$

where μ is the algorithm's step size (coefficient) that controls the convergence rate. Superscript * for the complex-conjugate of the vector. The small value of μ leads to a slow convergence rate. The large value of μ causes the algorithm to degrade the performance of the filter.

Therefore, selecting a step size is very important. The LMS algorithm has a simple structure and easy implementation with low computational complexity, but the disadvantages of LMS equations (9)-(10) are a fixed step size for every iteration. Finally, the instantaneous frequency f_k can be estimated as (Farhang-Boroujeny, 2013; Mandic and Goh, 2009; Manolakis *et al.*, 2000):

$$f_k = \frac{1}{2\pi\Delta T}\sin^{-1}\left(\Im\left(\underline{W_k}\right)\right) \tag{9}$$

where $\Im(.)$ represents the imaginary part of a complex-valued number. In NLMS, the step size is proportional to the inverse of total energy for the instantaneous values of the input vector V_k. The step size of the NLMS algorithm is updated by the following equation (18):

$$\mu_k = \frac{\mu}{||\underline{V_k}||_2^2} \tag{10}$$

where μ_k is time-varying ($0 < \mu_k < 2$) and μ is selected constant value.

To avoid division by 0 for small values of input $||\underline{V_k}||_2$ (Farhang-Boroujeny, 2013), a small "regularization" parameter ε is added to NLMS structure:

$$\mu_k = \frac{\mu}{||\underline{V_k}||_2^2 + \varepsilon} \tag{11}$$

3. The variable regularization–normalized least mean squares algorithm

The constant regularization parameter ε may lead to a low convergence rate of the NLMS algorithm. Parameter ε can be updated based on the gradient adaptive method (Jenkins *et al.*, 2012) as:

$$\varepsilon_k = \varepsilon_{k-1} - \eta \frac{\partial J_k}{\partial \varepsilon_{k-1}} \tag{12}$$

where J_k is the cost function ($J_k = \frac{1}{2}e_k^2 = \frac{1}{2}\underline{e_k}\underline{e_k^*}$), and η is step size parameter.

Computing the gradient:

$$\frac{\partial J_k}{\partial \varepsilon_{k-1}} = \frac{1}{2}\left(\underline{e_k}\frac{\partial \underline{e_k^*}}{\partial \varepsilon_{k-1}} + e_k^*\frac{\partial \underline{e_k}}{\varepsilon_{k-1}}\right) = \Re\left(\underline{e_k}^*\frac{\partial \underline{e_k}}{\partial \varepsilon_{k-1}}\right) \tag{13}$$

where $\Re$ implies the real component:

$$\frac{\partial \underline{e_k}}{\partial \varepsilon_{k-1}} = -\underline{V_k}^T\frac{\partial \underline{W_k}}{\partial \varepsilon_{k-1}} \tag{14}$$

and

$$\frac{\partial \underline{W_k}}{\partial \varepsilon_{k-1}} = -\frac{\mu\, \underline{e_{k-1}}\, \underline{V_{k-1}}^*}{\left(||\underline{V_{k-1}}||_2^2 + \varepsilon_{k-1}\right)^2} \tag{15}$$

Using the equations (13), (14) and (15) in equation (12), results in:

$$\varepsilon_k = \varepsilon_{k-1} - \eta \frac{\mu \Re\left(\underline{e_k}^* e_{k-1}\underline{V_k}^T\underline{V_{k-1}}^*\right)}{\left(||\underline{V_{k-1}}||_2^2 + \varepsilon_{k-1}\right)^2} \tag{16}$$

The detail steps of this VR-NLMS algorithm are shown in Figure 1.

In addition, the VR-NLMS algorithm may be concluded according to Frequency estimation using the VR-NLMS algorithm:

Downloaded by SHAHED UNIVERSITY OF MEDICAL SCIENCES, Ms Seyed Reza Aali At 05:58 02 November 2018 (PT)

Downloaded by SHAHED UNIVERSITY OF MEDICAL SCIENCES, Ms Seyed Reza Aali At 05:58 02 November 2018 (PT)

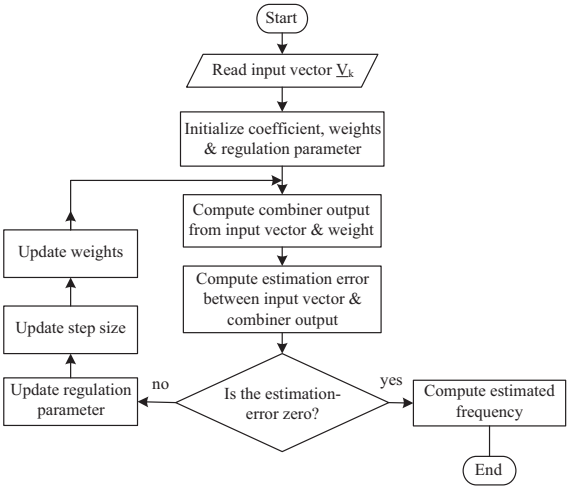

Figure 1.
Block diagram of the VR-NLMS

Parameters:
Coefficient $\{\eta, \mu\}$
Initialization:
$\varepsilon_0 = 0.001$
$W_0 = 0$
Available data:
Three-phase voltage signal $\{v_{a,k}, v_{b,k}, v_{c,k}\}$
Algorithm:
For $k = 1, 2, 3, ..., N$ do
Construct $\underline{V_k}$ using (3)

$$\underline{e_k} = \underline{V_k} - \underline{\hat{V}_k}$$

$$\varepsilon_k = \varepsilon_{k-1} - \eta \frac{\mu \Re\left(\underline{e_k}^* \underline{e_{k-1}} \underline{V_k}^T \underline{V_{k-1}}^*\right)}{\left(||\underline{V_{k-1}}||_2^2 + \varepsilon_{k-1}\right)^2}$$

$$\mu_k = \frac{\mu}{||\underline{V_k}||_2^2 + \varepsilon_k}$$

$$\underline{W_k} = \underline{W_{k-1}} + \mu_k \underline{e_{k-1}} \underline{V_{k-1}^*}$$

$$\underline{\hat{V}_k} = \underline{W_{k-1}} . \underline{\hat{V}_{k-1}}$$

$$\hat{f}_k = \frac{1}{2\pi\Delta T} \sin^{-1}\left(\Im\left(\underline{W_k}\right)\right)$$

End
Output:
Estimated frequency $\hat{f}_k$

4. Stability analysis of the variable regularization–normalized least mean squares algorithm

The theoretical stability analysis of the proposed algorithm is presented in this section. In the VR-NLMS algorithm, the weight vector $\underline{W_k}$ is updated according to the following equation:

$$\underline{W_k} = \underline{W_{k-1}} + \frac{\mu}{||\underline{V_k}||_2^2 + \varepsilon_k} \underline{e_{k-1}} \underline{V_{k-1}^*} \tag{17}$$

The function $V_{Ly} = |\underline{e_k}|$ is considered for stability analysis of this algorithm, and we have:

$$\begin{aligned} \Delta V_{Ly} &= |\underline{e_k}| - |\underline{e_{k-1}}| = |\underline{d} - \underline{V_k^T}\,\underline{W_k}| - |\underline{e_{k-1}}| \\ &= |\underline{d} - \underline{V_k^T}\{W_{k-1} + \frac{\mu}{||\underline{V_k}||_2^2 + \varepsilon_k} \underline{e_{k-1}}\,\underline{V_{k-1}^*}\}| - |\underline{e_{k-1}}| \end{aligned} \tag{18}$$

where d is the desire signal.

Then,

$$\Delta V_{Ly} = |\alpha - V_k^T \frac{\mu}{||V_k||_2^2 + \varepsilon_k} e_{k-1} V_{k-1}^*| - |e_{k-1}| \tag{19}$$

where $\alpha = \underline{d} - \underline{V_k^T}\,\underline{W_{k-1}}$.

On the other hand, we have (Mengüç and Acir, 2015; Zhang *et al.*, 2017):

$$\mu\, \underline{e_{k-1}} = \alpha - \kappa |\underline{e_{k-1}}| \operatorname{sign}(\alpha); \quad 0 \le \kappa < 1 \tag{20}$$

Therefore, equation (19) can be rewritten as:

$$\begin{aligned} \Delta V_{Ly} &= |\alpha - \underline{V_k^T}\,\underline{V_{k-1}^*} \frac{1}{|\underline{V_k}|_2^2 + \varepsilon_k} \left(\alpha - \kappa |\underline{e_{k-1}}| \operatorname{sign}(\alpha)\right)| - |\underline{e_{k-1}}| \\ &\approx |\alpha - \|\underline{V_k}\|^2 \frac{1}{|\underline{V_k}|_2^2 + \varepsilon_k} \left(\alpha - \kappa |\underline{e_{k-1}}| \operatorname{sign}(\alpha)\right)| - |\underline{e_{k-1}}| \le |\alpha \\ &- \left(\alpha - \kappa |\underline{e_{k-1}}| \operatorname{sign}(\alpha)\right)| - |\underline{e_{k-1}}| \end{aligned} \tag{21}$$

where $||\underline{V_k}||_2$ is L_2-norm of $\underline{V_k}$ that has a positive value and implies:

$$\Delta V_{Ly} = |\kappa |\underline{e_{k-1}}| \operatorname{sign}(\alpha)| - |\underline{e_{k-1}}| = -(1-\kappa)|\underline{e_{k-1}}| \Rightarrow \Delta V_{Ly} < 0 \tag{22}$$

The result, $\Delta V_{Ly} < 0$, means that the error $\underline{e_k}$ converges to zero, which proves the stability of the proposed estimation algorithm.

5. Variable regularization with a positive sequence extraction–normalized least mean squares algorithm

When dealing with signals that are unknown and operate in a wide range, applying a fixed regularization parameter ε may degrade the NLMS algorithm convergence and performance. To solve these problems, the regularization parameter ε should be variable.

The fixed regularization with a positive sequence extraction (FRP)-NLMS operates with a constant parameter of regularization ($\varepsilon_k = \varepsilon$) and DSC pre-filtering. This regularization parameter has small positive value to avoid the normalization with the division to zero.

Figure 2 shows the structure of the proposed strategy for the estimation of the fundamental frequency. The structure of the proposed variable regularization with a positive sequence extraction (VRP)-NLMS consists of three parts; Clarke's transformation, VR-NLMS algorithm and $\alpha\beta - DSC$ part. Three-phase voltage is converted into a two-phase complex using Clarke's transformation into a zero-sequence v_0 and the direct (v_α) and

Downloaded by SHAHED UNIVERSITY OF MEDICAL SCIENCES, Ms Seyed Reza Aali At 05:58 02 November 2018 (PT)

Downloaded by SHAHED UNIVERSITY OF MEDICAL SCIENCES, Ms Seyed Reza Aali At 05:58 02 November 2018 (PT)

quadrature-axis (v_β) components according to equation (2). The VRP-NLMS algorithm operates as explained in frequency estimation using the VR-NLMS algorithm described in Section 3. The $\alpha\beta - DSC$ part of the $\alpha\beta$-frame (complex) eliminates harmonic components by summing with their delayed versions. The DSC operator extracts FFPS component in the stationary reference frame according to the following equations (16, 26- 28):

$$\underline{V^{+}_{\alpha\beta,1}}(t) = \frac{1}{2}\left(\underline{V_{\alpha\beta}}(t) + e^{\frac{j2\pi}{n}}\underline{V_{\alpha\beta}}(t - T/n)\right) \tag{23}$$

where $\underline{V_{\alpha\beta}}(t) = V_\alpha(t) + jV_\beta(t)$ is the voltage vector in the $\alpha\beta$-frame, $\underline{V^{+}{}_{\alpha\beta,1}}(t) = V^{+}_{\alpha,1}(t) + j\,V^{+}_{\beta,1}(t)$ is the separated FFPS-voltage vector, $T = 1/f$ is the nominal value of the voltage fundamental period and n is the delay coefficient.

The Laplace domain of the $\alpha\beta - DSC$ operator is defined as:

$$DSC_n(s) = \frac{\underline{V^{+}{}_{\alpha\beta,1}}(s)}{\underline{V_{\alpha\beta}}(s)} = \frac{1 + e^{\frac{j2\pi}{n}}e^{-\frac{T}{n}s}}{2} \tag{24}$$

which DSC_n operator determines nth disturbance components of the voltage. Substituting $s = j\omega$ in the DSC operator implies that:

$$\begin{aligned} DSC_n(j\omega) &= |\cos\left(\frac{\omega T}{2n} - \frac{\pi}{n}\right)|\angle - \left(\frac{\omega T}{2n} - \frac{\pi}{n}\right) \\ &= |\cos\left(\frac{\pi h}{n} - \frac{\pi}{n}\right)|\angle - \left(\frac{\omega T}{2n} - \frac{\pi}{n}\right) \end{aligned} \tag{25}$$

Figure 3 shows the definition of the DSC block with nth time delay factor in a time domain. The DSC_n block can eliminate certain sets of harmonics, for example, $n = 4$, $|DSC_4(h)| = 0$ satisfies for $h = 4k - 1$ which means DSC_4 will eliminate all $4k - 1$($k = \pm1, \pm2, \pm3,\ldots$) order harmonics in the grid voltage. Also, for $n = 12$, $|DSC_{12}(h)| = 0$ satisfies for $h = 12k + 1$ and DSC_{12} eliminate all $12k + 1$ order harmonics in the grid voltage.

Most often a single DSC operator is not enough to eliminate all harmonic components. Therefore, several DSCoperators hybrid series form with special delay factors are used. Equation (26) describes the $\alpha\beta - DSC$ operator in s-domain where m is the number of cascaded $\alpha\beta - DSC$ operators:

$$\begin{aligned} &DCS_{n_1,n_2,\ldots n_m}(s) = \\ &DCS_{n_1}(s).DCS_{n_2}(s)\ldots.DCS_{n_m}(s) \end{aligned} \tag{26}$$

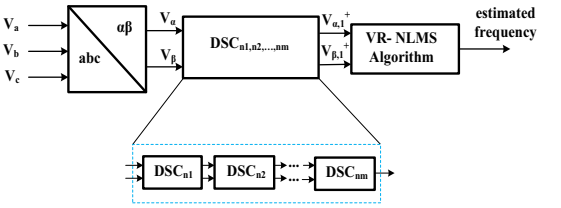

Figure 2.
Schematic diagram of DSC operator-based VRP-NLMS

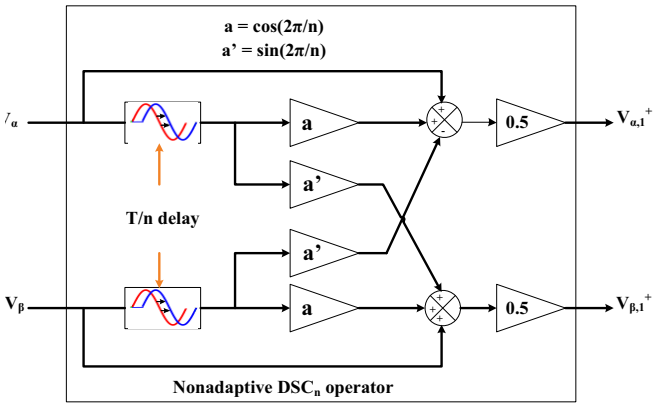

Figure 3.
Time domain implementation of the DSC_n operator

The multiple cascaded-DSC operators extract the fundamental-frequency or positive-sequence component effectively (Zhang *et al.*, 2017; Wang and Li, 2011a, 2011b).

6. Simulation results and discussions

Figure 4 shows the frequency response of the $DSC_{4,4,12,12,24,24}$ operator (Golestan *et al.*, 2017) in cascade together. The frequency response of the filter is approximately flat about 50 Hz and separate fundamental-frequency positive-sequence component of the voltage from the negative sequence and harmonics.

Replacing $s = j\omega_g$ into equation (25), where ω_g is the fundamental frequency, gives the phase and magnitude of the DSC operator at the fundamental frequency as:

$$\angle DSC_{4,4,12,12,24,24}(j\omega_g) = -\sum_{n=4,4,12;12;24;24}\left(\frac{\omega_g T}{2n} - \frac{\pi}{n}\right) \tag{27}$$

$$|DSC_{4,4,12,12,24,24}(j\omega_g)| = \prod_{n=4,4,12,12,24,24}\left|\cos\left(\frac{\omega_g T}{2n} - \frac{\pi}{n}\right)\right| \tag{28}$$

Defining $\omega_g = \omega_0 + \Delta\omega_g$, where $\omega_0 = {}^{2\pi}/_{T}$ is the nominal value of the frequency and $\Delta\omega_g$ denotes the deviation of the grid frequency from its nominal valueand replacing it into equations (27) and (28) obtains:

$$\angle DSC_{4,4,12,12,24,24}(j\omega_g) = -\sum_{n=4,4,12,12,24,24}\left(\frac{\Delta\omega_g T}{2n}\right) = -k_\varphi \Delta\omega_g \tag{29}$$

$$\begin{aligned}|DSC_{4,4,12,12,24,24}(j\omega_g)| &= \prod_{n=4,4,12,12,24,24}\left|\cos\left(\frac{\Delta\omega_g T}{2n}\right)\right| \\ &\approx \prod_{n=4,4,12,12,24,24}\left(1 - \left(\frac{\Delta\omega_g T}{2n}\right)^2/2\right) \approx 1 - k_a(\Delta\omega_g)^2\end{aligned} \tag{30}$$

Downloaded by SHAHED UNIVERSITY OF MEDICAL SCIENCES, Ms Seyed Reza Aali At 05:58 02 November 2018 (PT)

Downloaded by SHAHED UNIVERSITY OF MEDICAL SCIENCES, Ms Seyed Reza Aali At 05:58 02 November 2018 (PT)

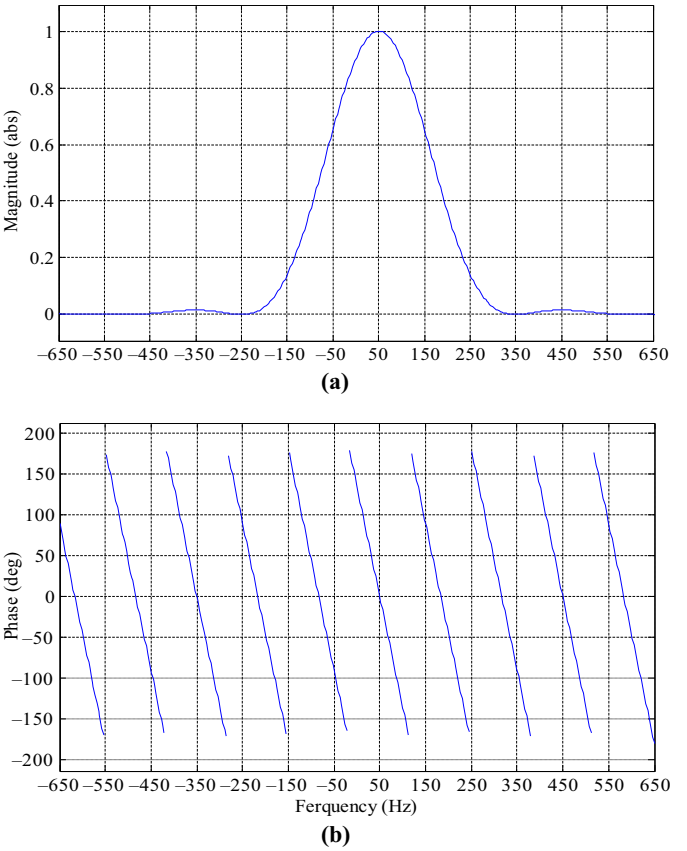

Figure 4.
Frequency response (a) magnitude; and (b) phase of the $DSC_{4,4,12,12,24,24}$ operators

where $k_\varphi = \frac{T}{2}\left(\sum_{n=4,4,12,12,24,24}\frac{1}{n}\right)$ and $k_a = \frac{T^2}{8}\left(\sum_{n=4,4,12,12,24,24}\frac{1}{n^2}\right)$.

Therefore, equations (29), (30) show the phase and amplitude of DSC around the fundamental frequency (50 Hz). The $DSC_{4,4,12,12,24,24}$ operator eliminates symmetrical and asymmetrical harmonics in grid voltage.

Simulations were performed in the Matlab programing environment with a sampling rate of 20 kHz, and the step-size μ of all NLMS algorithms was set to be 0.01. Also, the step-size parameter of η was set to be 0.1 in all simulations. The electrical system consists of a 25-kV voltage source with 100 MVA short-circuit level, and 100 kVA three-phase power transformers, transmission lines 30 km in length that feeds load of 33 kW. Power transformers have a star connection in the high voltage winding and a star connection in the low voltage winding.

6.1 Frequency estimation under unbalance voltage

Type C voltage sags are one kind of unsymmetrical voltage sags that originate from line-to-line fault. Figure 5 shows a phasor view of Type C voltage sags. The balanced system became unbalanced after the fault. The fault occurs in the vicinity of the load before

Downloaded by SHAHED UNIVERSITY OF MEDICAL SCIENCES, Ms Seyed Reza Aali At 05:58 02 November 2018 (PT)

transformer with a resistance of 2 Ω, and it is caused about a 20 per cent drop and 15° phase angles offset for phases V_b and V_c. The real-imaginary curves convert from circularity (balance) to non-circularity of Clarke's voltage in unbalanced conditions.

The DSC pre-filter suppresses the asymmetric component of the measured voltage in the phasor domain and non-circularity of Clarke's voltage is changed to circularity voltage as VR-NLMS input.

The negative-sequence and zero-sequence components illustrate the imbalance between the three voltages; the zero-sequence is in many cases blocked by the transformers. A voltage dip is characterized by a relationship between the positive-sequence voltage and the negative-sequence voltage. The zero-sequence component is not used in the estimation of frequency in the NLMS algorithm. Therefore, the only zero-sequence component of the voltage has no effect on the proposed-estimation algorithm.

In addition, the hybrid DSC operator with PLL (DSC-PLL) presented in Golestan *et al* (2017) is compared with the proposed algorithm. The DSC operator extracts the positive component of the voltage. This positive voltage is given to NLMS with variable regulation in VRP-NLMS. The estimator's performance in the presence of Type C voltage sags is carried out with the simulation presented in Figure 6, and the numeric results are exposed in Table I. The sag is occurring in $t = 1$ to 1.2 sec. The simulation is divided into two zones: in Zone 1 and Zone 2. Zone 1 is extended from $t = 1$ to 1.2 sec, and Zone 2 is the time larger than 1.2 sec. The positive sequence of voltage is separated by DSC in FRP and VRP-NLMS. Therefore, these algorithms are stable where the FR-NLMS and VR-NLMS estimators cannot handle the disturbance in steady state, exhibiting an error greater than 10 Hz. The FRP and VRP-NLMS track the reference frequency under distortions. The VRP-NLMS has shorter settling times with minimum error. Hence, time-varying regularization of the NLMS shows a better dynamic response and a smart operation under Type C voltage sags.

The normalized mean square deviation (NMSD) is used as an index for quality evaluation of the adaptive filter. It evaluates the accuracy and convergence rate which is defined as (Sayed, 2003):

$$NMSD = 10\log_{10}\left(\frac{||f - \hat{f}||_2^2}{||\hat{f}||_2^2}\right) \tag{31}$$

NMSD is used to show the performance of the estimation with respect to the convergence rate and steady-state misalignment. The NMSD curves for this sort of voltage sags are shown in Figure 7 with different NLMS algorithms and DSC-PLL during the first 1.5 sec.

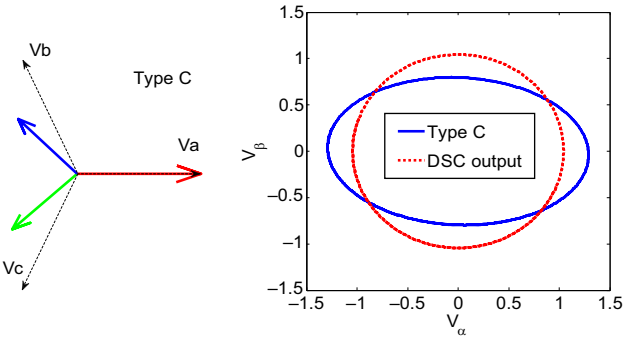

Figure 5. Steady-state trajectory in an alpha-beta plane (right) and the phasor (left) views of Type C voltage sags

Downloaded by SHAHED UNIVERSITY OF MEDICAL SCIENCES, Ms Seyed Reza Aali At 05:58 02 November 2018 (PT)

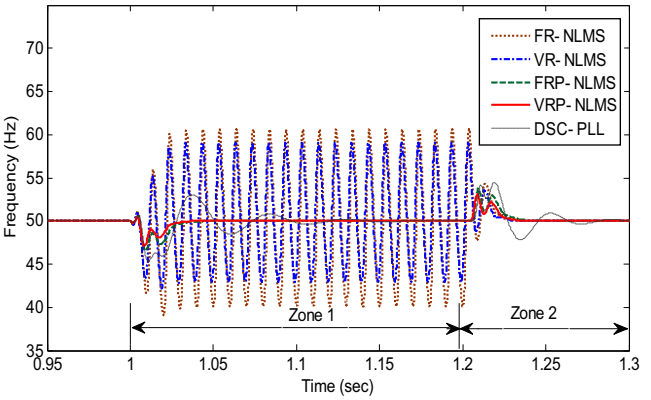

Figure 6.
Frequency estimation for Type C voltage sags with different NLMS algorithms and DSC-PLL

	Settling time (ms)	Maximum error (Hz) Transient	Steady state
Zone 1			
FR-NLMS	∞	9.92	9.89
VR-NLMS	∞	9.31	9.29
FRP-NLMS	41	3.51	0
VRP-NLMS	33	3.05	0
DSC PLL	162	4.77	0
Zone 2			0
FR-NLMS	45	10.47	0
VR-NLMS	37	9.45	0
FRP-NLMS	40	3.72	0
VRP-NLMS	34	3.16	0
DSC PLL	295	4.77	0

Table I.
Measurements from Figure 6

Initial transient condition effects on NMSD curves before first 1 sec. The three-phase voltage arrived in the steady-state condition in the vicinity of 0.8 sec, and fault occurs at $t = 1$ to 1.2 sec. The VRP-NLMS algorithm exhibits the best performance among the others in transient conditions.

If the voltage sags of Type C pass through a delta/y transformer, it will be converted to Type D voltage sags. The phasor view of Type D voltage sags, having about 20 per cent voltage drop at the line V_a and a 10 per cent voltage drop on both V_b and V_c with a 5° phase angle offset as illustrated in Figure 8. This fault also leads balanced system to an unbalanced system. The non-circularity of Clarke's voltage is changed to circularity voltage. The DSC output fed VR-NLMS and PLL to improve the operation of these measurements.

Figure 9, Table II and Figure 10 indicate frequency estimation and NMSD curves for Type D voltage sags with different methods. The FR-NLMS and VR-NLMS have the worst performance with the settling times and with the maximum errors. The DSC-PLL has a slow convergence rate with a bad performance ratio than the FRP and VRP-NLMS. Hence, it is observed that the proposed algorithm provides a high-efficient estimation with the best performance and low steady-state misalignment compared with the other algorithms.

Downloaded by SHAHED UNIVERSITY OF MEDICAL SCIENCES, Ms Seyed Reza Aali At 05:58 02 November 2018 (PT)

6.2 Frequency estimation under harmonic voltage

The 6-pulse delta/y and delta/delta connected rectifiers as nonlinear loads are connected to the tested distribution system at $t = 1$ to 1.2 sec. The grid voltage is polluted with harmonics and total harmonic distortion (THD) of the voltage is 13.12 per cent. Figure 11 shows geometric and the phasor views of voltage harmonics under three-phase to ground fault (balance). Also, the real–imaginary plots illustrate the non-circularity of Clarke's voltage in harmonic condition.

Frequency estimation, numeric results and NMSD curves under voltage harmonics with different NLMS algorithms and DSC-PLL is shown in Figure 12, Table III and Figure 13, respectively. The simulation is divided into two zones: in Zone 1, the voltage is instantaneously polluted, and in Zone 2, the voltage recovers from the disturbance instantaneously. In Zone 1, the FR-NLMS and the VR-NLMS have steady-state errors greater than 4 Hz. As such, the settling times for these estimators are infinite. In Zone 1, the steady-state error of the FRP-NLMS, VRP-NLMS and DSC PLL are zero because of the operation of the DSC.

Also, the FR-NLMS and VR-NLMS estimators have the greater transient error. The VRP-NLMS and the FRP-NLMS strategies have similar responses to the lower transient

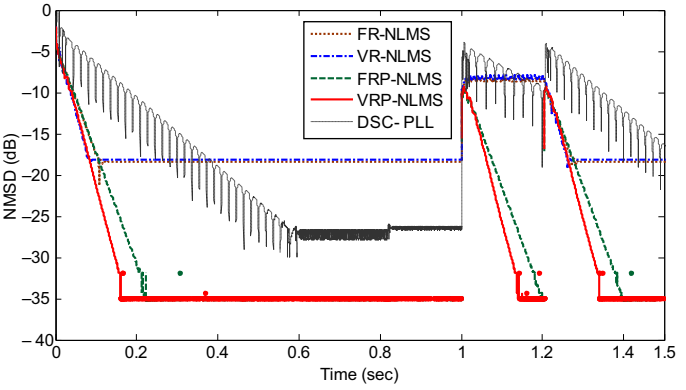

Figure 7.
NMSD curves for Type C voltage sags with different NLMS algorithms and DSC-PLL

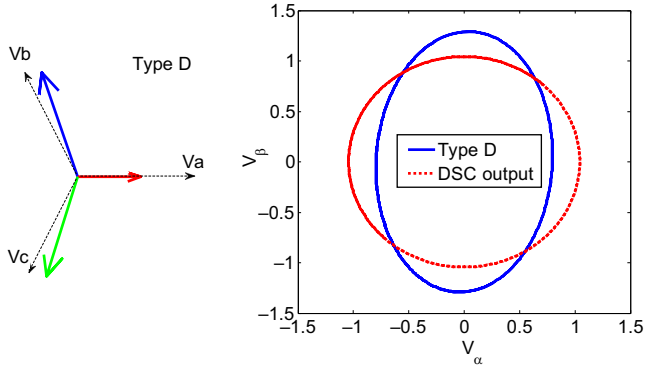

Figure 8.
Steady-state trajectory in the alpha-beta plane (right) and the phasor (left) views of Type D-unbalanced voltage sags

Downloaded by SHAHED UNIVERSITY OF MEDICAL SCIENCES, Ms Seyed Reza Aali At 05:58 02 November 2018 (PT)

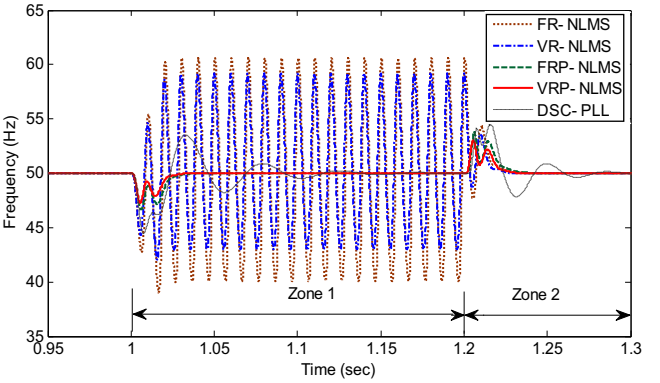

Figure 9.
Frequency estimation for Type D voltage sags with different NLMS algorithms and DSC-PLL

	Settling time (ms)	Maximum error (Hz) Transient	Steady state
Zone 1			
FR-NLMS	∞	10.05	10.03
VR-NLMS	∞	9.25	9.22
FRP-NLMS	24	3.43	0
VRP-NLMS	21	3.75	0
DSC PLL	110	5.62	0
Zone 2			0
FR-NLMS	35	10.08	0
VR-NLMS	28	9.12	0
FRP-NLMS	31	3.95	0
VRP-NLMS	22	3.34	0
DSC PLL	82	4.53	0

Table II.
Measurements from Figure 9

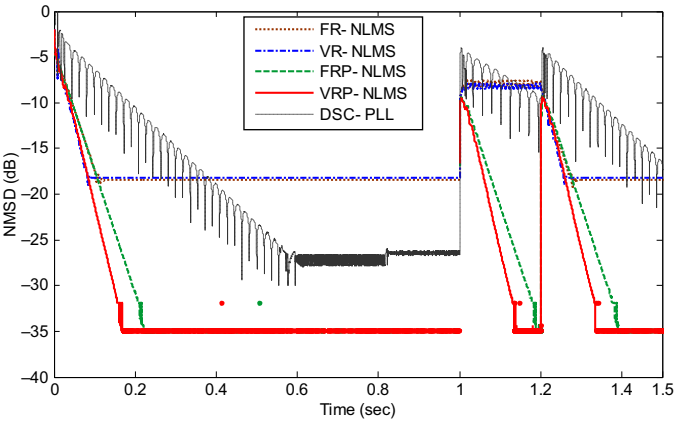

Figure 10.
NMSD curves for Type D voltage sags with different NLMS algorithms and DSC-PLL

error. The accuracy and the speed of the estimation have a very satisfactory behavior with VRP-NLMS in the presence of harmonics.

Sub-harmonics are defined as non-integer harmonics with the frequency below the main fundamental under consideration. The corresponding waveform of the grid voltage is shown Figure 14 (left) and polluted with a sub-harmonics component of 10 per cent of amplitude and 2.5 Hz frequency. Also, it is polluted with 10 per cent of 3th inter-harmonics and 10 per cent of 5th inter-harmonics, simultaneously.

The performance of the proposed and conventional-frequency estimation under sub- and inter-harmonics is shown in Figure 15. The VRP-NLMS strategy has steady state errors less than 0.1 Hz. As it can be observed, the proposed technique is less sensitive to the presence of harmonics as compared to the other methods. The proposed estimator has robust again sub- and inter-harmonics.

6.3 Frequency estimation under frequency deviations

Figure 16a illustrates the superior performance of the VRP-NLMS estimator for a power system in the presence of a grid frequency step. The reference frequency is decreased to 49.8 Hz at $t = 1$ sec, and it is recovered to the previous value at $t = 1.1$ sec. The estimation speed and accuracy by VRP-NLMS algorithm is more than other methods.

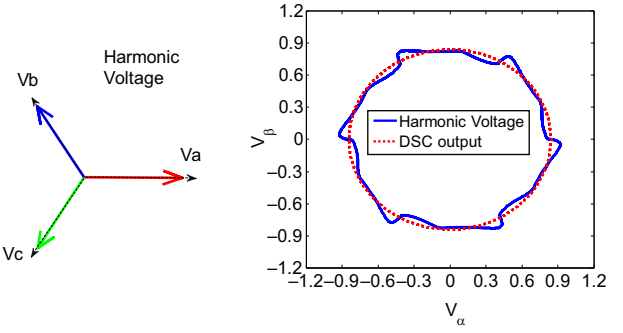

Figure 11. Steady-state trajectory in the alpha-beta plane (right) and phasor (left) views of voltage harmonics

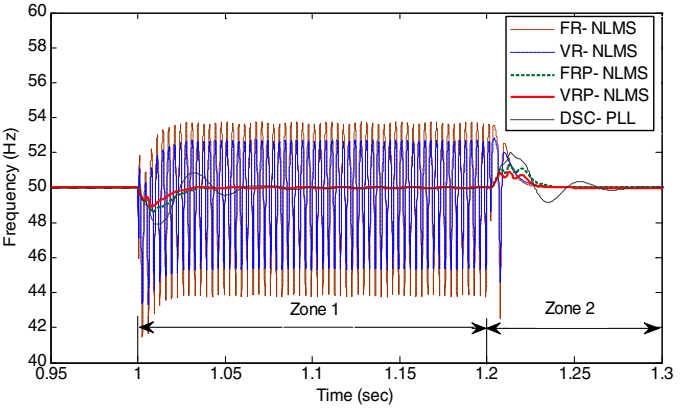

Figure 12. Frequency estimation for voltage harmonics with different NLMS algorithms and DSC-PLL

Downloaded by SHAHED UNIVERSITY OF MEDICAL SCIENCES, Ms Seyed Reza Aali At 05:58 02 November 2018 (PT)

Downloaded by SHAHED UNIVERSITY OF MEDICAL SCIENCES, Ms Seyed Reza Aali At 05:58 02 November 2018 (PT)

	Settling time (ms)	Maximum error (Hz) Transient	Steady state
Zone 1			
FR-NLMS	∞	8.48	7.95
VR-NLMS	∞	7.36	4.87
FRP-NLMS	25	3.43	0
VRP-NLMS	21	3.75	0
DSC PLL	73	5.62	0
Zone 2			
FR-NLMS	34	7.15	0
VR-NLMS	31	5.22	0
FRP-NLMS	29	1.17	0
VRP-NLMS	26	0.93	0
DSC PLL	89	2.05	0

Table III.
Measurements from Figure 12

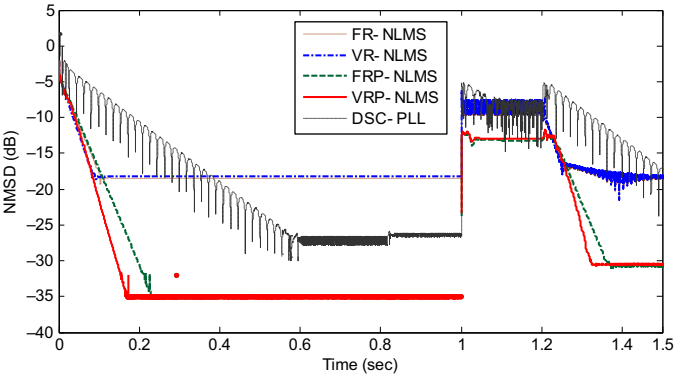

Figure 13.
NMSD curves for voltage harmonics with different NLMS algorithms and DSC-PLL

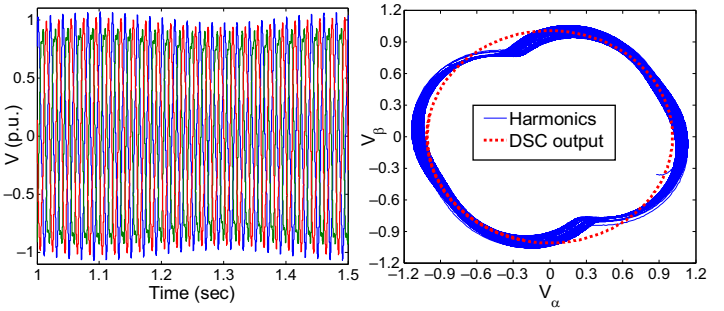

Figure 14.
The Steady-state trajectory in the alpha-beta plane (right) and the phasor (left) views of sub-and inter-harmonics in time domain

7. Conclusion

In this paper, a new NLMS-based DSC is proposed to estimate and track the frequency of the power system. The simulation results validated the analytical findings under different conditions such as voltage sags, unbalance and harmonic distortions and frequency variations. The proposed algorithm exhibits a considerably improved convergence rate and

Downloaded by SHAHED UNIVERSITY OF MEDICAL SCIENCES, Ms Seyed Reza Aali At 05:58 02 November 2018 (PT)

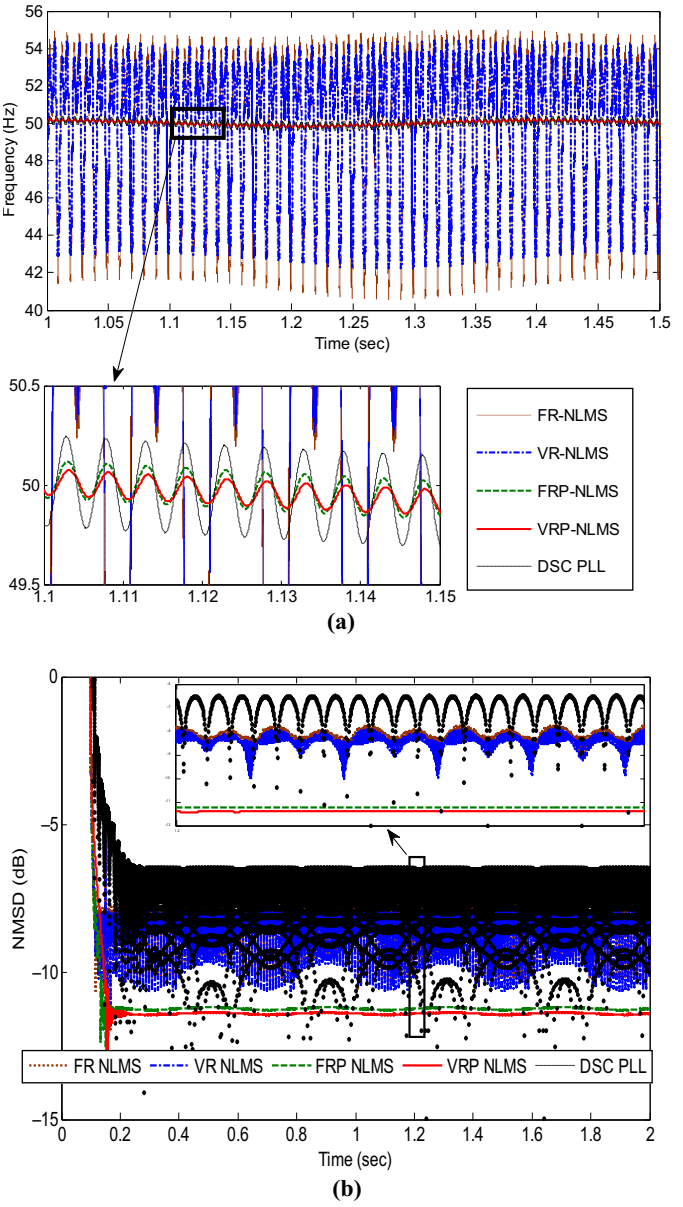

Figure 15.
(a) Frequency estimation; and (b) NMSD curves for voltage sub- and inter-harmonics with different NLMS algorithms and DSC-PLL

tracking properties relative to the other existing NLMS methods. A DSC operator is placed before the NLMS algorithm in the proposed estimator. The positive sequence of voltage is separated by the DSC operator in FRP and VRP-NLMS algorithms. The DSC operator in the FRP and VRP-NLMS algorithms operates as pre-filter, and it extracts the fundamental component of the voltage, and it is caused to low misalignment with the best performance.

Downloaded by SHAHED UNIVERSITY OF MEDICAL SCIENCES, Ms Seyed Reza Aali At 05:58 02 November 2018 (PT)

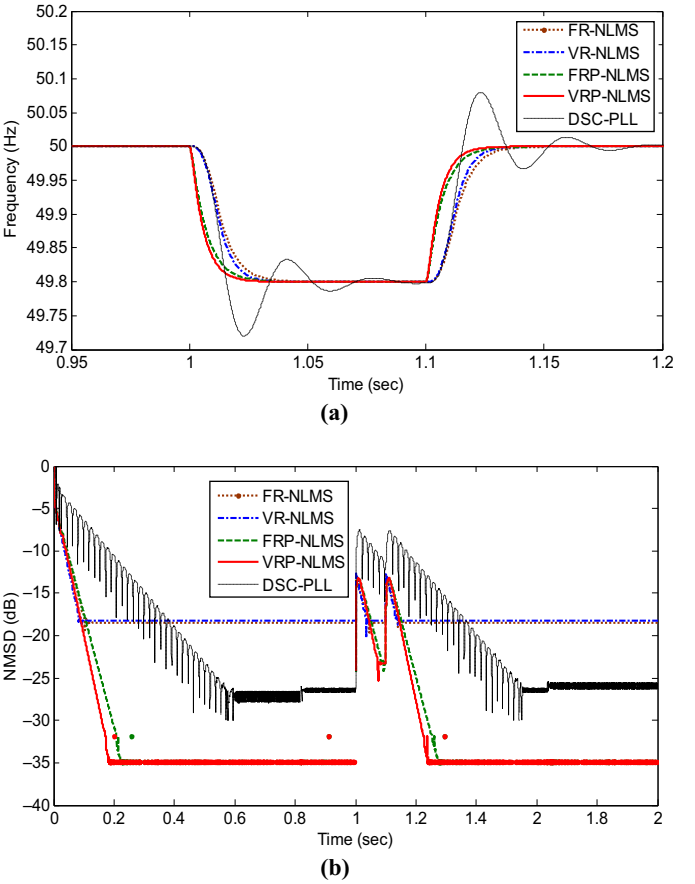

Figure 16.
(a) Frequency estimation; and (b) NMSD curves for frequency step with different NLMS algorithms and DSC-PLL

The VRP-NLMS algorithm is smarter than the FRP-NLMS algorithm because of VR. The VR varies the step size of the estimation. The proposed step size has adaptive value and reduces the tradeoff between maladjustment and tracking ability of the fixed step size NLMS algorithm. The variable step size algorithm also reduces the sensitivity of the maladjustment to the level of non-stationarity. Also, the proposed algorithm has been compared with DSC-PLL; the proposed algorithm is stable and immune to the disturbance. The VRP-NLMS has the best performance and fast convergence rate.

References

Arablouei, R., Doğançay, K. and Werner, S. (2015), "Adaptive frequency estimation of Three-Phase power systems", *Signal Processing*, Vol. 109, pp. 290-300.

Bei, T.-Z. and Wang, P. (2016), "Robust Frequency-Locked loop algorithm for grid synchronization of Single-Phase applications under distorted grid conditions", *IET Generation, Transmission and Distribution*, Vol. 10 No. 11, pp. 2593-2600.

Downloaded by SHAHED UNIVERSITY OF MEDICAL SCIENCES, Ms Seyed Reza Aali At 05:58 02 November 2018 (PT)

Chellappa, R. and Theodoridis, S. (2014), *Signal Processing Theory and Machine Learning*, Academic Press.

Chilipi, R.R., Al Sayari, N., Beig, A.R. and Al Hosani, K. (2016), "A multitasking control algorithm for Grid-Connected inverters in distributed generation applications using adaptive noise cancellation filters", *IEEE Transactions on Energy Conversion*, Vol. 31 No. 2, pp. 714-727.

Ciobotaru, M., Agelidis, V.G., Teodorescu, R. and Blaabjerg, F. (2010), "Accurate and Less-Disturbing active antiislanding method based on PLL for Grid-Connected converters", *IEEE Transactions on Power Electronics*, Vol. 25 No. 6, pp. 1576-1584.

Dash, P.K., Panda, G., Pradhan, A., Routray, A. and Duttagupta, B. (2000), "An extended complex kalman filter for frequency measurement of distorted signals", *Power Engineering Society Winter Meeting, Conference Proceedings* (Cat. No.00CH37077).

Dini, D.H. and Mandic, D.P. (2013), "Widely linear modeling for frequency estimation in unbalanced Three-Phase power systems", *IEEE Transactions on Instrumentation and Measurement*, Vol. 62 No. 2, pp. 353-363.

Farhang-Boroujeny, B. (2013), *Adaptive Filters: Theory and Applications*, John Wiley and Sons.

Golestan, S., Guerrero, J.M. and Vasquez, J.C. (2017), "Hybrid adaptive/nonadaptive delayed signal Cancellation-Based Phase-Locked loop", *IEEE Transactions on Industrial Electronics*, Vol. 64 No. 1, pp. 470-479.

Golestan, S., Ramezani, M., Guerrero, J.M. and Monfared, M. (2015), "Dq-Frame Cascaded delayed signal Cancellation-Based PLL: Analysis, design, and comparison with moving average Filter-Based PLL", *IEEE Transactions on Power Electronics*, Vol. 30 No. 3, pp. 1618-1632.

He, W., Yuan, X. and Hu, J. (2017), "Inertia provision and estimation of PLL-Based dfig wind turbines", *IEEE Transactions on Power Systems*, Vol. 32 No. 1, pp. 510-521.

Huang, Q. and Rajashekara, K. (2017), "An improved delayed signal cancellation PLL for fast grid synchronization under distorted and unbalanced grid condition", *IEEE Transactions on Industry Applications*, Vol. 53 No. 5, pp. 4985-4997.

Jenkins, W.K., Hull, A.W., Strait, J.C., Schnaufer, B.A. and Li, X. (2012), *Advanced Concepts in Adaptive Signal Processing*, Springer Science and Business Media.

Li, Y., Tang, G., An, T., Pang, H., He, Z. and Wu, Y. (2017), "A control strategy of frequency Self-Adaptation without Phase-Locked loop for VSC-HVDC", *CSEE Journal of Power and Energy Systems*, Vol. 3 No. 2, pp. 131-139.

Mandic, D.P. and Goh, V.S.L. (2009), "Complex valued nonlinear adaptive filters: Noncircularity", *Widely Linear and Neural Models*, John Wiley and Sons.

Manolakis, D.G., Ingle, V.K. and Kogon, S.M. (2000), *Statistical and Adaptive Signal Processing: Spectral Estimation, Signal Modeling, Adaptive Filtering, and Array Processing*, McGraw-Hill Boston.

Mengüç, E.C. and Acir, N. (2015), "A Complex-Valued adaptive filter algorithm for system identification problem", in, *9th International Conference on Electrical and Electronics Engineering (ELECO)*.

Sayed, A.H. (2003), *Fundamentals of Adaptive Filtering*, John Wiley and Sons [Database][Mismatch]

Simon, H. (2002), "Adaptive filter theory", *Prentice Hall*, pp. 478-481.

Smith, J.C., Thresher, R., Zavadil, R., DeMeo, E., Piwko, R., Ernst, B. and Ackermann, T. (2009), "A mighty wind", *IEEE Power and Energy Magazine*, Vol. 7 No. 2, pp. 41-51.

Subudhi, B., Ray, P.K., Mohanty, S. and Panda, A. (2009), "A comparative study on different power system frequency estimation techniques", *International Journal of Automation and Control*, Vol. 3 Nos 2/3, pp. 202-215.

Wang, Y.F. and Li, Y.W. (2011a), "Analysis and digital implementation of cascaded Delayed-Signal-Cancellation Pll", *IEEE Transactions on Power Electronics*, Vol. 26 No. 4, pp. 1067-1080.

Wang, Y.F. and Li, Y.W. (2011b), "Grid synchronization PLL based on cascaded delayed signal cancellation", *IEEE Transactions on Power Electronics*, Vol. 26 No. 7, pp. 1987-1997.

Xia, Y. and Mandic, D.P. (2012), "Widely linear adaptive frequency estimation of unbalanced Three-Phase power systems", *IEEE Transactions on Instrumentation and Measurement*, Vol. 61 No. 1, pp. 74-83.

Xia, Y., He, Y., Wang, K., Pei, W., Blazic, Z. and Mandic, D.P. (2017), "A complex least squares enhanced smart DFT technique for power system frequency estimation", *IEEE Transactions on Power Delivery*, Vol. 32 No. 3, pp. 1270-1278.

Zhang, S., So, H.C., Mi, W. and Han, H. (2017), "A family of adaptive decorrelation NLMS algorithms and its diffusion version over adaptive networks", *IEEE Transactions on Circuits and Systems I: Regular Papers*, Vol. 65 No. *2*, pp. 638-649.

Further reading

de Souza, H.E., Bradaschia, F., Neves, F.A., Cavalcanti, M.C., Azevedo, G.M. and de Arruda, J.P. (2009), "A method for extracting the Fundamental-Frequency Positive-Sequence voltage vector based on simple mathematical transformations", *IEEE Transactions on Industrial Electronics*, Vol. 56 No. *5*, pp. 1539-1547.

Golestan, S., Freijedo, F.D., Vidal, A., Yepes, A.G., Guerrero, J.M. and Doval-Gandoy, J. (2016), "An efficient implementation of generalized delayed signal cancellation pll", *IEEE Transactions on Power Electronics*, Vol. 31 No. *2*, pp. 1085-1094.

Corresponding author

Mohammad Reza Besmi can be contacted at: Besmi@shahed.ac.ir

Downloaded by SHAHED UNIVERSITY OF MEDICAL SCIENCES, Ms Seyed Reza Aali At 05:58 02 November 2018 (PT)

For instructions on how to order reprints of this article, please visit our website:
www.emeraldgrouppublishing.com/licensing/reprints.htm
Or contact us for further details: **permissions@emeraldinsight.com**